ATMOSPHERIC SCIENCE LETTERS
Atmos. Sci. Let. **18**: 342–348 (2017)
Published online in Wiley Online Library
(wileyonlinelibrary.com) **DOI:** 10.1002/asl.762

RMetS
Royal Meteorological Society

Energetics of wave propagation leading to frost events in South America: extratropical latitudes

Gabriela V. Müller,[1]* Manoel Alonso Gan[2] and Everson Dal Piva[3]

[1] *Centro de Investigaciones Científicas y Transferencia de Tecnología a la Producción (CICYTTP/CONICET), Consejo Nacional de Investigaciones Cientificas y Tecnicas, Diamante, Argentina*
[2] *Centro de Previsão de Tempo e Estudo Climáticos, Instituto Nacional de Pesquisas Espaciais (CPTEC/INPE), São José dos Campos, Brazil*
[3] *Departamento de Física, Centro de Ciências Naturais e Exatas, Universidade Federal de Santa Maria (UFSM), Santa Maria, Brazil*

**Correspondence to:*
G. V. Müller, Centro de Investigaciones Científicas y Transferencia de Tecnología a la Producción (CICYTTP/CONICET), Consejo Nacional de Investigaciones Cientificas y Tecnicas, Materi y España, s/n, CP 3105, Diamante, Entre Ríos, Argentina.
E-mail:
gabrielamuller@cicyttp.org.ar

Received: 8 January 2017
Revised: 23 May 2017
Accepted: 27 June 2017

Abstract

The dynamics of wave propagation and energy associated with frosts in extratropical versus tropical South American latitudes is studied. A double wave train propagates through the southern hemisphere following the polar and subtropical jets. If, in the previous day, both trains coincide in phase over the southeast Pacific (southwest Atlantic) Oceans, it will contribute to generate generalized frosts (strong frosts) at extratropical (tropical) latitudes, not affecting tropical (extratropical) latitudes given the wave train zonal propagation. The vertically averaged eddy kinetic energy composites show three maxima associated with those trains over the South Pacific Ocean and South American region.

Keywords: **frosts; Rossby wave patterns; energetics; South America**

1. Introduction

There are just few studies about the energetics of tropical latitudes for extreme cold events. Krishnamurti *et al.* (1999) made a decomposition of the waves associated to the frost events in the southeast of Brazil, in waves of synoptic scale that propagates eastward and planetary waves that possess an almost-stationary characteristic. Using the prognostic data of a high-resolution global model it is seen that the growth of the stationary long wave was due to the wave interaction in different time and space scales, e.g. wave/wave interaction during the frost events. They also observed in this energetics study that interactions of non-linear barotropic scales are also important sources of energy to maintain the average amplification. Despite the fact that the baroclinic instability was observed as the main source of kinetic energy, Krishnamurti *et al.* (1999) associated the amplification of the mid-latitude upper level trough to the mechanism of downstream development (DSD) proposed by Orlanski and Katzfey (1991) for cyclonic waves in the Southern Hemisphere.

Recently, Müller *et al.* (2015) investigated the cold and cool frost events, which affect the tropical latitudes of South America, considering the energetics of the wave train propagation associated to such events. The energetics shows that the cold events kinetic energy maxima are more intense than those of cool events. For the cold events three maxima are observed, the first (K1) and the third (K3) maxima are developed by baroclinic conversion and ageostrophic flux convergence and the second one (K2) by ageostrophic flux convergence. For the cool events two maxima are found, the first maximum (K4) developed by baroclinic conversion and the second one (K5) by ageostrophic flux convergence. In both types of frost events, the intensification of the wave is associated with ageostrophic flux convergence. These results are in agreement with Krishnamurti *et al.* (1999).

This paper studies the energetics of the wave trains associated with the GF in extratropical latitudes of South America, and the results are compared with the extreme cold events in tropical latitudes of South America of Müller *et al.* (2015). With the purpose of providing forecast tools for the occurrence of extreme cold events in South America, we compare the propagation of wave patterns associated with extreme cold events in the extratropics versus those associated with same type of events in the tropics of the region.

2. Event selection criteria, data and methodology

The meteorological stations selected are situated in central-east Argentina, known as wet Pampas (27°–40°S and 65°–57°W). In particular, Generalized Frosts (GF) are defined as those where the area with temperatures below or equal to 0 °C surpasses 75% of the meteorological stations in the region. In this

Table 1. Events selected from the MJJAS with generalized frosts with 1 SD above average.

Generalized frost events
24 June 1970, 7 July 1970, 8 August 1970, 25 August 1970
12 June 1974, 22 July 1974, 7 August 1974, 16 August 1974, 1 September 1974
11 June 1976, 26 June 1976, 4 July 1976, 14 August 1976
1 June 1988, 14 June 1988, 24 June 1988, 5 July 1988, 24 July 1988, 26 August 1988

study, the GF that are taken to represent cold outbreaks are those events which took place during years of maximum frequency of GF occurrence. They were selected following the criteria defined by Müller *et al.* (2005), who selected those periods when the number of frosts is 1 SD (Standard Deviation) unit below or above the mean value for the period 1961–1990.We considered this period because is the one with better information and larger number of meteorological stations available in the region of analysis. The same period was used in different Müller's studies, so that it will serve for comparison of results with this study. The criterion is applied to the months between May and September, considering those years above the mean, i.e. years of maximum frequency of occurrence of GF in the wet Pampas. The resulting years 1970, 1974, 1976, 1988, consider a minimum time interval of 7 days in a sequence of days with GF, and the selected dates are shown in Table 1. In this way, each day represents a single synoptic situation associated to cold outbreaks affecting extratropical latitudes.

A composite analysis of the frost events (Table 1) to study the wave train propagation during the days previous to GF is done using the NCEP/NCAR reanalysis (Kalnay *et al.* 1996). The results are tested by applying the Student's *t*-test.

The energetics of the frost event composites is studied through the Eddy Kinetic Energy (EKE) equation (Equation (1)) developed by Orlanski and Katzfey (1991) and modified by Chang (2000). Although some researcher used the formulation of the Lorenz (1967) as Pezza *et al.* (2010, 2014), we prefer the energetics analysis that was recently applied by Müller *et al.* (2015) for tropical frost events over South America and Gan and Piva (2013, 2016) for cut-off lows, because this equation separates the energy transport and leaves a transport term that can be directly associated with downstream development (DSD) proposed by Orlanski and Katzfey (1991)

$$\frac{\partial \mathrm{EKE}}{\partial t} = -\nabla.\vec{V}\mathrm{EKE} - \nabla.\overrightarrow{V'_a}\varphi' - \omega'\alpha' - \vec{V'}.\left(\overrightarrow{V'_3}.\nabla_3\right)\overline{\vec{V}} + \vec{V'}.\overline{\left(\overrightarrow{V'_3}.\nabla_3\right)\vec{V'}} - \frac{\partial}{\partial p}\omega\mathrm{EKE} - \frac{\partial}{\partial p}\omega'\varphi' + \mathrm{RES} \quad (1)$$

In Equation (1), α is the specific volume, $\vec{V}$ is the two-dimensional horizontal wind, $\vec{V'}$ the 2D eddy wind, $\vec{V_3}$ the 3D wind, $\overrightarrow{V'_3}$ the 3D eddy wind, $\overrightarrow{V'_a}$ the 2D eddy ageostrophic wind, p_s the surface pressure and φ' is the eddy geopotential. The subscript "3" in the operators indicates three-dimensional vectors and the overbar denotes a 91-day time mean centered (45 days before and 45 days after) every 6 h for each frost case. The prime means deviation from the 91-day time mean.

The term on the left hand side of Equation (1) is the local tendency of EKE. The first term on the right hand side represents the EKE flux convergence (KFC), the second term is the ageostrophic flux convergence (AFC) and the third term is the baroclinic conversion (BRC). The fourth and fifth terms are due to Reynold's stresses and can be regarded as barotropic conversion (BRT) terms. The sixth and seventh terms are the vertical flux convergence of energy. The term RES contains, among other things, mechanisms not explained by Equation (1), such as friction, diabatic effects and sub-grid fluxes, as well as errors introduced by numerical methods. To analyze the Equation (1) terms, we made a vertical weighted averaging from the first isobaric level located above the ground to the 100 hPa level.

3. Results

3.1. Wave train propagation

The composites of 300 hPa meridional wind anomalies and their statistical significance of the GF events presented in Table 1, are shown in Figure 1. In this figure we see a double Rossby wave train that is driven by the zonal flow. One reaches the continent in subtropical latitudes, and the other is close to polar latitudes. These two wave trains propagate independently along the two jets and they merge in a single perturbation extending meridionally, the day before the GF event. The anomaly circulation pattern contributes to the advection of polar air over the continent. This pattern is similar to that observed prior to the event in winters (JJA) with most frequent GF events (Müller *et al.* 2005), as well in the most persistent ones (Müller and Berri, 2007) and very persistent GF event (Müller and Berri 2012). In other words, the most frequent events and those of greatest persistence in winter, are caused by the propagation of a wave pattern that does not follow the classical behavior of a single Rossby wave train, rather they are generated by a double wave train which coincides in phase before its entrance into the continent prior to the event. These results were confirmed through numerical experiments and linear wave theory done by Müller and Ambrizzi (2007). Using a basic state of GF maximum frequency of occurrence, they simulated the double wave train which propagates along the southern hemisphere driven by the subtropical and polar jets, with a

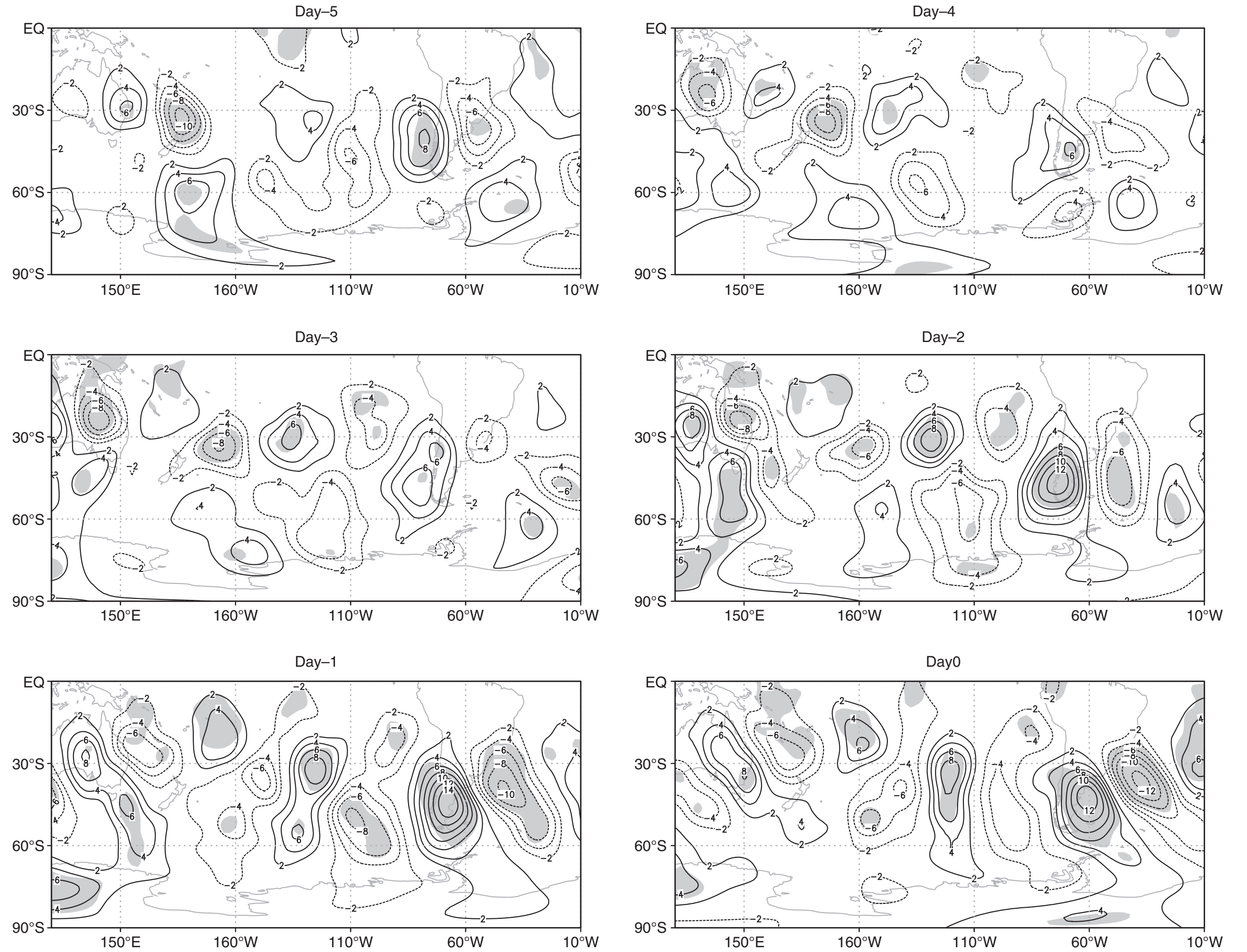

Figure 1. Meridional wind composites anomaly (m s^{-1}) from day −5 to day 1 at 300 hPa, corresponding to GF events. Positive (negative) contours are shown in solid (dashed) lines every 2 m s^{-1}. The shaded areas indicate regions with 95% confidence level according to a Student's *t*-test.

phase coincidence to the west of the Andes. As suggested by the authors, the winters with maximum frequency of occurrence show a subtropical jet with maximum values around 30°S extending from the Indian Ocean to the Pacific Ocean and reaching the South American continent. At high latitudes the polar jet position was also different from the climatology (winter JJA 1961–1990) indicating an extension towards South America.

On the other hand Müller *et al.* (2015) found for low latitude cool outbreaks of strong event composites, a wave train that propagates following the subtropical jet, which is joined by a second less intense wave train, which propagates along the polar jet in the western Atlantic Ocean on day 0 (Figure 3, Müller *et al.*, 2015). They have a zonal propagation and on the lee side of the Andes Mountains they merge into a unique wave train that due to its meridional orientation will favor cold air advection affecting the oriental coast of South America. These conditions that contribute to cooling the air and the later entrance of the anticyclone from the west-southwest, driven by the observed wave train, enhance radiative loss, temperature drop and the observed frosts.

3.2. Energetics

The evolution of the vertically averaged EKE for all cases along the wave train observed in the GF composite shows that on day −2 (Figure 2(a)) there are three kinetic energy maxima (K1, K2 and K3). K1 over South Pacific Ocean around 130ºW–67ºS, K2 close to the southeastern of South America and K3 is over the Andes Mountains around 40°S. On day −1.5 (figure not shown) K1 displaces eastward and weakens, K2 is slightly displaced to the west and intensified and K3 appears over the South American continent around central Argentina. K1 and K2 continue with a slow eastward movement until day 0 (Figure 2(c)) when these three kinetic energy maxima weaken while remaining over the coast of Argentina and Uruguay. The maximum intensity of K1 occurs on day −2.5 (figure not shown), the maximum intensity of K2 occurs on day −1 (Figure 2(b)) and K3 on day −1.5 (figure not shown). As we can see in Figure 2(b), K2 and K3 are associated with the wave that contributed to the GF and they are located in the region between the ridge and the trough.

The baroclinic conversion term has a positive contribution to K1, K2 and K3 maxima during the analyzed

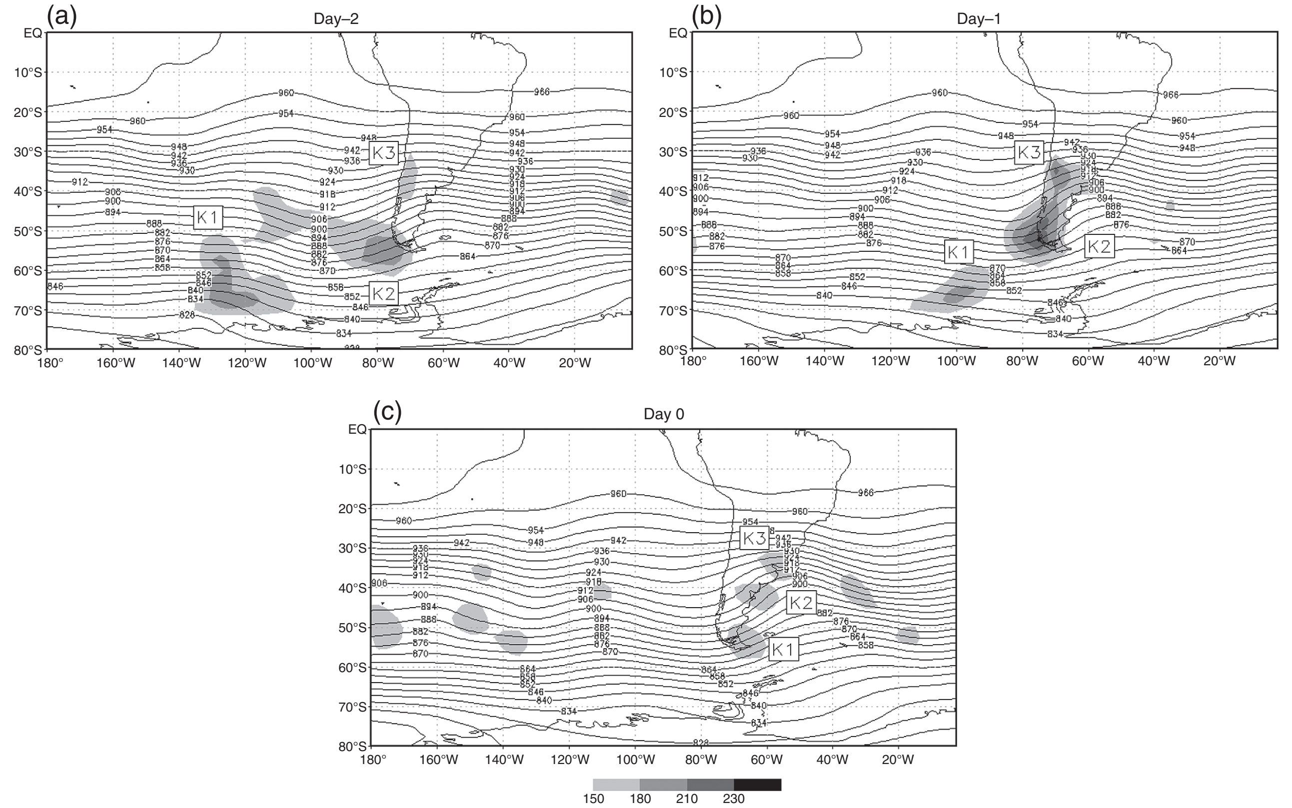

Figure 2. The 300 hPa geopotential height ($\times 10\,m^2\,s^{-2}$), with three regions of maximum vertically averaged eddy kinetic energy (shaded), identified as K1, K2 and K3, for day −2 (a), day −1 (b) and day 0 (c) of the GF composite.

period (Figures 3(a)–(c)), keeping the disturbance intensification all the time through the conversion of potential into eddy kinetic energy. This result shows that baroclinic instability is important to maintain these kinetic energy maxima. The barotropic term (Figures 3(d)–(f)) has a different behavior for each kinetic energy maximum. This term has a negative contribution to K1, i.e. converting eddy kinetic energy into zonal kinetic energy from day −2 to day −1 (Figures 3(d) and (e)), after which this term is positive (Figure 3(f)). However, for K2 this conversion term has a positive contribution until day 0 (Figures 3(d)–(f)), meaning that this energy maximum could be sustained by conversion of zonal kinetic energy into eddy kinetic energy. On day −2 when K3 appears, this term is close to zero, meaning that K3 intensified by other processes (Figure 3(d)). On day −1 this term has a negative contribution (Figure 3(e)) and on day 0 the contribution is positive (Figure 3(f)).

The ageostrophic flux fields (Figures 4(a) to (c)) show the existence of an area of strong fluxes extending from the south Pacific (near 70°S; 160°W) to South America, crossing the three EKE maxima on day −2 and day −1 (Figures 4(a) and (b)). This area of strong fluxes has associated with it areas of convergence and divergence (Figures 4(d)–(f)), indicating the downstream propagation of eddy energy. In the downstream propagation associated with ageostrophic fluxes it is common to notice a convergence and divergence on west and east sides of the EKE maximum, respectively. This is what happens for the K1 and K2 maxima, but not for the K3. In the latter, there is only divergence throughout the event explaining why the EKE has not increased. The AFC term seems to be important for the growth of K2, because AFC is positive and above $180\,m^2\,s^{-2}\,day^{-1}$ near the center of it (Figure 4(e)).

In addition, we observed a bifurcation in ageostrophic fluxes on the south Pacific-South America area mainly on days −2 and −1 (Figures 4(a) and (b)). This bifurcation explains the negative area of AFC over South America, indicating divergence of energy flows (Figures 4(d)–(e)). The ageostrophic fluxes bifurcation and the divergence of the AFC coincide with the merge of the two wave trains previously pointed out when discussing Figure 1.

The energetics of the GF composites shows a different behavior when we compare it with the cool and cold frost composite of tropical latitudes studied by Müller *et al.* (2015). A main characteristic is that the intensity of the EKE maxima associated with the frost events is lower in the GF cases in extratropical than in tropical latitudes. This is because in the tropical case the Rossby wave has more amplitude and the zonal wind anomaly is more intense when compared with extratropical GF cases.

Another difference between the energetics of frost in these two regions is that the cold cases have three maxima, with the first and the third maximum developed by baroclinic conversion and ageostrophic flux

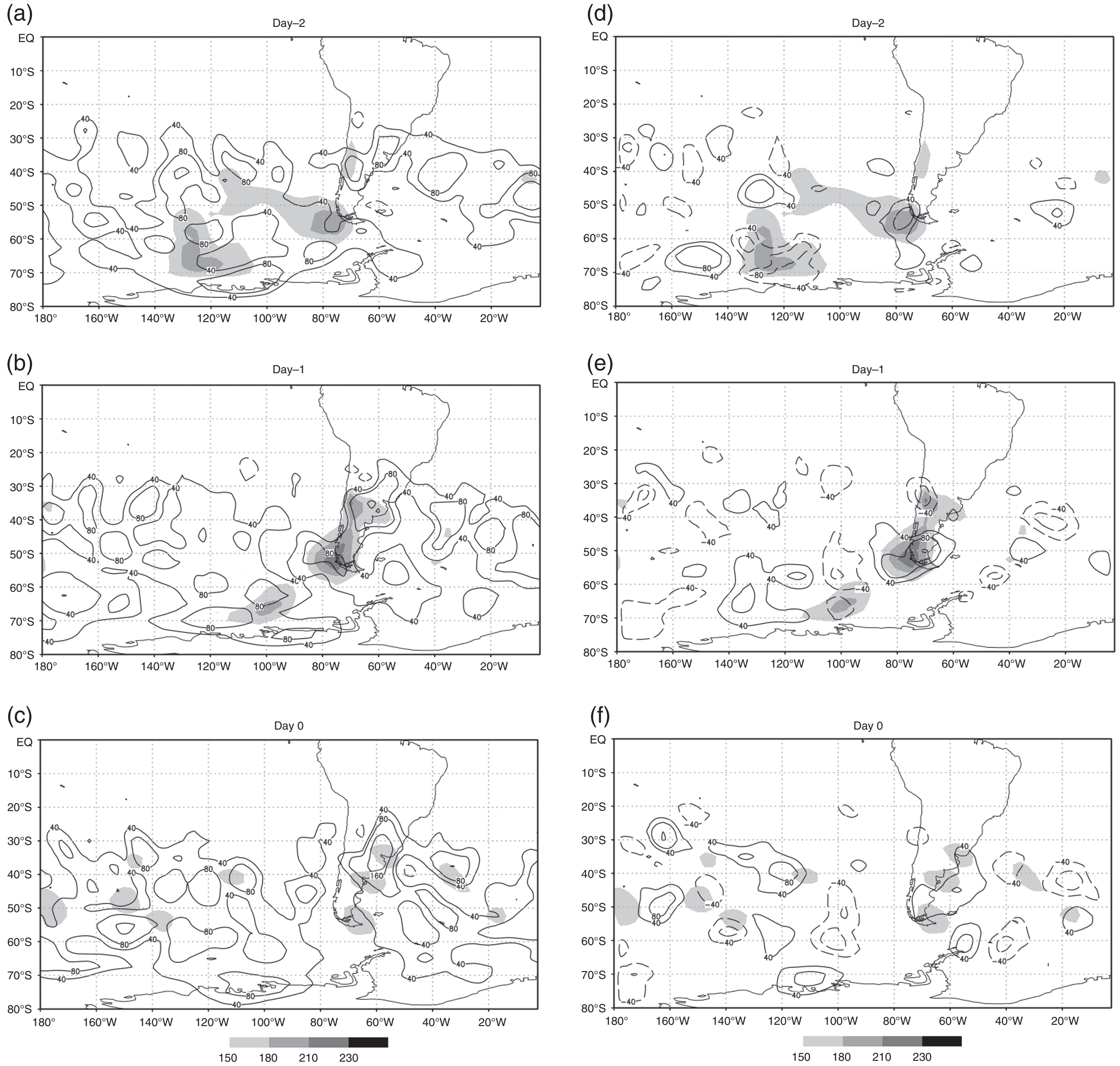

Figure 3. Vertically averaged BRC term for day −2 (a), day −1 (b) and day 0 (c) of the GF composite. Vertically averaged BRT term for day −2 (d), day −1 (e) and day 0 (f) of the GF composite. The contour interval is 2×10^{-2} m^2 s^{-2} day −1, zero line omitted and positive (negative) contours in continuous (dashed) lines. The shaded areas are the regions of maximum vertically averaged eddy kinetic energy.

convergence and the second one by ageostrophic flux convergence.

A similarity is that, the cool events have two maxima acting directly, one developing by baroclinic conversion and the other by AFC, as happened in the extratropical GF.

4. Conclusions

The analysis of wet Pampa GF events composites, representative of the extratropical latitudes, shows a double wave train which propagates along the subtropical and subpolar jets in the south Pacific Ocean, prior to a GF event in the wet Pampa, whose phases coincide to the west of the continent causing an extended and intense advection of polar air over the whole southern cone. This result agrees with those obtained in the case of GF events during winters with maximum frequency of occurrence by Müller and Ambrizzi (2007), and the most and very persistent GF events (Müller and Berri, 2007, 2012, respectively). The results suggest that the phase coincidence of the waves propagating along the subtropical and polar jets is an important precondition for favoring extreme events. If this coincidence is observed in the southeast Pacific Ocean, it will contribute to generate GF events at extratropical latitudes and it will not affect the tropical latitudes, given the zonal propagation of the wave train. However, if the phase coincidence takes place in the southwest Atlantic Ocean, extreme cool events will occur at

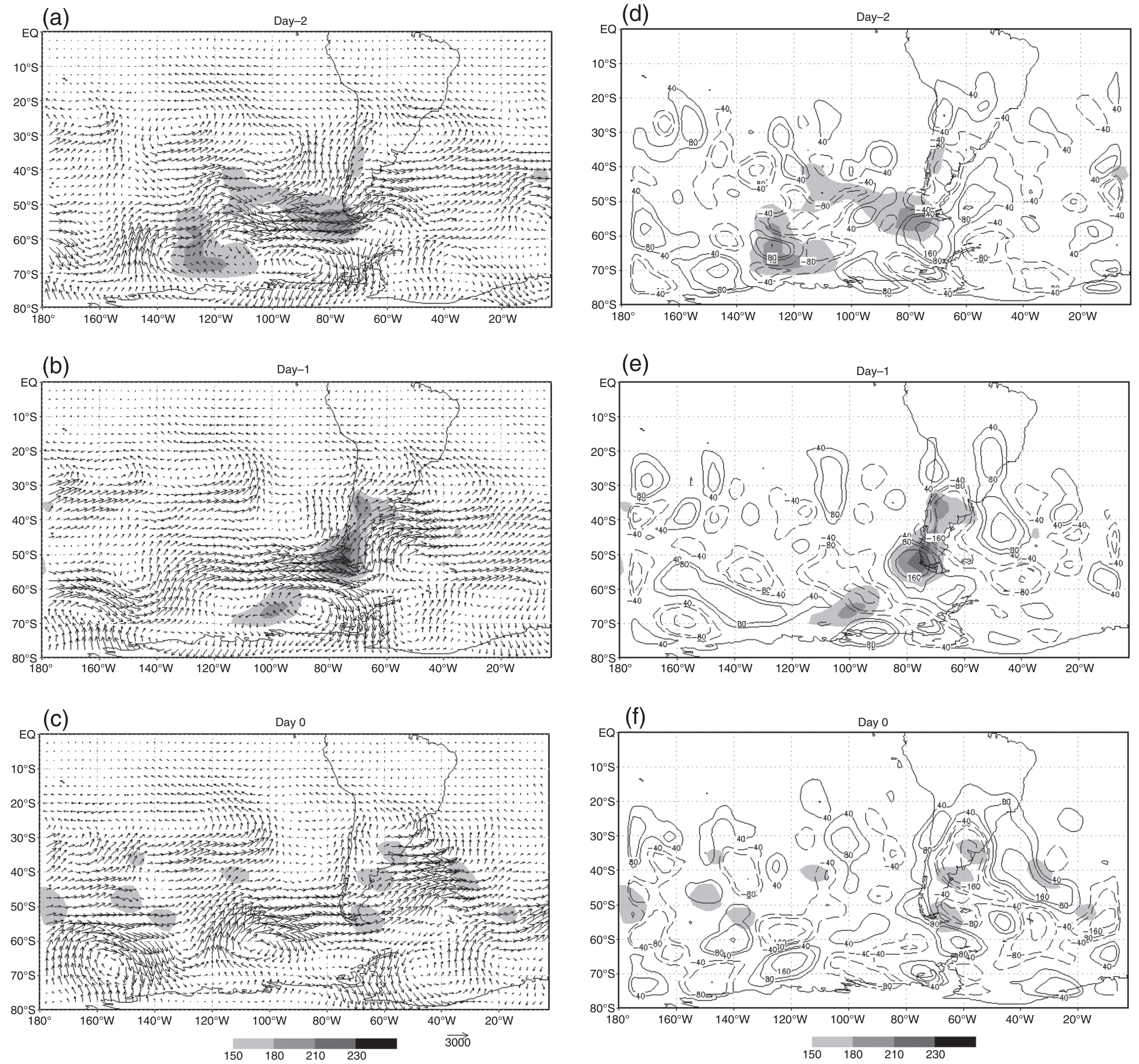

Figure 4. Ageostrophic flux (in units of $m^2\ s^{-3}$, see arrow below panel) for day −2 (a), day −1 (b) and day 0 (c) of the GF composite. Vertically averaged AFC term for day −2 (d), day −1 (e) and day 0 (f) of the GF composite. The contour interval is $2\times10^{-2}\ m^2\ s^{-2}$ day −1, zero line omitted, and positive (negative) contours in continuous (dashed) lines. The shaded areas are the regions of maximum vertically averaged eddy kinetic energy.

tropical latitudes, with no impacts on extratropical ones. The phase and location of the wave train are very important not only for frost event but also to other events like extreme heat waves and rainfall events such as that occurred in eastern of Australia described by Boschat *et al.* (2015) when a Rossby wave amplification over the south Indian and Pacific Oceans induced a quasi-stationary blocking high system. The circulation associated with the high system advected hot and dry air to the area that recorded extreme heat wave event during the Australian's summer.

The vertically averaged eddy kinetic energy composites show three energy maxima associated with these wave trains over the South Pacific Ocean and South American region. The analysis of EKE shows two maxima (K2 and K3) located between the ridge and the trough of the wave over the continent on the day of the GF. The main source of eddy kinetic energy of the three maxima is the baroclinic conversion. K2 also has a positive contribution from barotropic conversion. The ageotrophic flux convergence term does not present a significant positive contribution, except on day −1 when this term is positive in most parts of the K2 region.

The results obtained here corroborate with the downstream baroclinic development mechanism discussed by Orlanski and Sheldon (1993) and Orlanski and Gross (2000). The authors state that disturbances in the middle or exit regions of the storm track tend to develop due to the ageostrophic fluxes convergence, while the disturbances at the entrance region of the storm tracks grow by baroclinic conversion. This seems to be the case of the K2 and K3, because K2 maximum develops (with AFC term important) at the end of the Pacific Storm track and the K3 maximum develops over the South America (in the beginning of Atlantic Storm tracks) region known to be frontogenetic (Satyamurty and Mattos, 1989; Arraut and Barbosa, 2009).

The energetics of the GF composites shows a different behavior when we compare it with the cool and cold frost composites to tropical latitudes studied by Müller *et al.* (2015). The intensity of the EKE maxima associated with the frost events in tropical latitudes is higher than in GF cases in the extratropical latitudes. This is because in the tropical case the Rossby wave has higher amplitude and the zonal wind anomaly is more intense when compared with the extratropical GF cases. Other difference is that the cold cases have three maxima, the first and the third maximum developed by baroclinic conversion and ageostrophic flux convergence and the second one by ageostrophic flux convergence.

As similarity, as in the case of GF composite the cool events have two maxima acting directly, one developing by baroclinic conversion and the other one by ageostrophic flux convergence.

For future studies to analyze the changes in eddy available potential energy are also important. As the current study showed that baroclinic conversion was important, considerable available potential energy changes are expected, because the baroclinic conversion is a conversion term between eddy available potential energy and EKE.

References

Arraut JM, Barbosa HMJ. 2009. Large scale features associated with strong frontogenesis in equivalent potential temperature in the South America subtropics east of the Andes. *Advances in Geosciences* **22**: 73–78.

Boschat G, Pezza A, Simmonds I, Perkins S, Cowan T, Purich A. 2015. Large scale and sub-regional connections in the lead up to summer heat wave and extreme rainfall events in eastern Australia. *Climate Dynamics* **44**: 1823–1840.

Chang EKM. 2000. Wave packets and life cycles of troughs in the upper troposphere: examples from the Southern Hemisphere summer season of 1984/85. *Monthly Weather Review* **128**: 25–50.

Gan MA, Piva ED. 2013. Energetics of a Southeastern Pacific cut-off low. *Atmospheric Science Letters* **14**: 272–280.

Gan MA, Piva ED. 2016. Energetics of southeastern Pacific cut-off lows. *Climate Dynamics* **46**: 3453–3462.

Kalnay E, Kanamitsu M, Kistler R, Collins W, Deaven D, Gandin L, Iredell M, Saha S, White G, Woollen J, Zhu Y, Celliah M, Ebisuzaki W, Higgins W, Janowiak J, Mo KC, Ropelewski C, Wang J, Leetmaa A, Reynolds R, Jenne RE, Joseph D. 1996. The NCEP/NCAR 40-year reanalysis project. *Bulletin of the American Meteorological Society* **77**: 437–471.

Krishnamurti TN, Tewari M, Chakraborty DR, Marengo JA, Silva Dias PL, Satyamurti P. 1999. Downstream amplification: a possible precursor to major freeze events over southeastern Brazil. *Weather and Forecasting* **14**: 242–270.

Lorenz EN. 1967. *The Nature and Theory of the General Circulation of the Atmosphere*. World Meteorological Organization: Geneva; 161.

Müller GV, Ambrizzi T. 2007. Teleconnection patterns and Rossby wave propagation associated to generalized frosts over southern South America. *Climate Dynamics* **29**: 633–645.

Müller GV, Ambrizzi T, Núñez MN. 2005. Mean atmospheric circulation leading to generalized frosts in central southern South America. *Theoretical and Applied Climatology* **82**: 95–112.

Müller GV, Berri GJ. 2012. Atmospheric circulation associated with extreme generalized frosts persistence in central-southern South America. *Climate Dynamics* **38**: 837–857.

Müller GV, Berri GJ. 2007. Atmospheric circulation associated with persistent generalized frosts in Central-Southern south America. *Monthly Weather Review* **135**: 1268–1289.

Müller GV, Gan MA, Dal Piva E, Piccinini VS. 2015. Energetics of wave propagation leading to cold event in tropical latitudes of South America. *Climate Dynamics* **45**: 1–20.

Orlanski I, Gross B. 2000. The life cycle of baroclinic eddies in a storm track environment. *Journal of the Atmospheric Science* **57**: 3498–3513.

Orlanski I, Katzfey J. 1991. The life cycle of a cyclone wave in the Southern Hemisphere. Part I: eddy energy budget. *Journal of the Atmospheric Sciences* **48**: 1972–1998.

Orlanski I, Sheldon J. 1993. A case of downstream Baroclinic development over Western North America. *Monthly Weather Review* **121**: 2929–2950.

Pezza AB, Garde LA, Veiga JAP, Simmonds I. 2014. Large scale features and energetics of the hybrid subtropical low 'Duck' over the Tasman Sea. *Climate Dynamics* **42**: 453–466.

Pezza AB, Veiga JAP, Simmonds I, Keay K. 2010. Environmental energetics of an exceptional high-latitude storm. *Atmospheric Science Letters* **11**: 39–45.

Satyamurty P, Mattos LF. 1989. Climatological lower tropospheric frontogenesis in the midlatitudes due to horizontal deformation and divergence. *Monthly Weather Review* **117**: 1355–1364.

